Available online at www.sciencedirect.com
ScienceDirect
Cement and Concrete Research 37 (2007) 579–588
Cement and Concrete Research

Experimental study of gas diffusion in cement paste

J. Sercombe [a,*], R. Vidal [a], C. Gallé [b], F. Adenot [a]

[a] Atomic Energy Commission, Cadarache, 13108 Saint-Paul-Lez-Durance, France
[b] Atomic Energy Commission, Saclay, 91191 Gif-sur-Yvette, France

Received 2 November 2005; accepted 6 December 2006

Abstract

This paper presents an experimental study of gas diffusion in binary mixtures of hydrogen–nitrogen and xenon–nitrogen through cement pastes (CEM I and CEM V) of different water/cement ratios (0.35 and 0.45). First, the impact of water saturation on gas diffusion is investigated by performing tests on samples pre-conditioned in specific atmospheric conditions (dry, 55, 70, 82, 93 and 100% RH) by means of saline solutions. The comparison of the results obtained for the CEM I and the CEM V samples (*w*/*c* ratio of 0.45) demonstrate the importance of pore size distribution/connectivity on gas diffusion. Second, diffusion tests at different total pressures and using two different mixtures (hydrogen–nitrogen, xenon–nitrogen) are performed to study the nature of gas diffusion in cement paste. Results demonstrate that gas diffusion in cement paste is controlled by Knudsen and ordinary diffusion at pressures greater than 100 kPa and mainly by Knudsen diffusion at pressures less than 100 kPa.

Keywords: Humidity; Microstructure; Diffusion; Transport properties; Cement paste; Hydrogen

1. Introduction

Durability of concrete structures often depends on the rate of ingress of gaseous or aqueous elements into the concrete porous network. Migration of gaseous elements in concrete can be driven by pressure or concentration gradients, i.e., by viscous flow or diffusion. Carbonation is a typical example where gas diffusion, i.e., carbon dioxyde, plays an important role with respect to the overall kinetics of the deterioration process [1–3]. Drying is another example where the kinetics of gas diffusion, i.e., vapour water diffusion, can be of some importance [4–6]. In consequence, many mathematical descriptions used to estimate these phenomena depend on the diffusion coefficient of gas species in the porous network of concrete.

Gas diffusion through porous media is often divided in three independent modes or mechanisms with a distinct diffusion coefficient for each of them [7]: free-molecule or Knudsen diffusion, molecular or ordinary diffusion and surface diffusion. Usually surface diffusion is neglected, mostly because it is basically an assumption which does not rest on experimental evidence. Theoretically, ordinary diffusion, in which the different species of a mixture move relative to each other under the influence of concentration gradients, occurs predominantly when molecule–molecule collisions dominate over molecule–pore wall collisions. On the contrary, Knudsen diffusion, in which molecules of different species move entirely independently of each other, occurs predominantly when molecule–molecule collisions can be ignored compared to molecule–pore wall collisions.

The prevalence of Knudsen or ordinary diffusion depends, first, on the mean free path of the gas molecule (approximately 0.1 μm for a gas molecule at atmospheric pressure and 20 °C) which depends itself on the total pressure, the temperature of the gas mixture and on the molecular weight of the gas species, second, on the size (diameter if the pores are assumed to be cylindrical) and degree of connectivity of the unsaturated pores (accessible to gas). Since the pore diameters in cement pastes, mortars or concretes are widely distributed from the nanometer to the millimeter scale, it is difficult to state, a priori, which is the dominant mechanism in cementitious materials.

Furthermore, the pore size distribution and degree of connectivity of the unsaturated pores in cementitious materials

* Corresponding author.
E-mail address: sercombe@cea.fr (J. Sercombe).

0008-8846/$ - see front matter © 2006 Published by Elsevier Ltd.
doi:10.1016/j.cemconres.2006.12.003

strongly rely on the mix-design properties (*w/c* ratio, type of cement, proportion of aggregates,…) and on the curing/conservation conditions (Relative Humidity, temperature, carbonation) which modify the moisture content and/or the water saturation (i.e., the percentage of the total pore volume filled with water) of the materials. In this respect, some studies have pointed out the importance of moisture content, *w/c* ratio, aggregate content, type of cement, curing/conservation conditions on the diffusion of gas through mortars or concretes [8–12].

In this paper, the impact of the moisture content, of the total porosity and pore size distribution, of the total gas pressure and of the gas molecular weight on gas diffusion in pure cement pastes is investigated experimentally. Hydrogen and xenon are used in the tests, mainly because they do not react with the pore structure of cement pastes and because they provide data for gases with large variations of properties. It is expected that the collected data can thus be extrapolated to other gases and therefore be used in the mathematical description of diffusion-based phenomena (carbonation, drying,…). Conclusions are given concerning the prevalence of Knudsen or ordinary diffusion at low to moderate pressures.

2. Modes of gas transport in porous media

Usually, four modes of gas transport can be considered in porous media [7], as illustrated schematically in Fig. 1. Three of them are related to concentration or partial pressure gradients (molecular diffusion, Knudsen diffusion, surface diffusion), and one to the total gas pressure gradient (viscous or bulk flow). In the discussion which follows, no total pressure gradient (no bulk flow) is considered since this is the condition which prevails in the experiments presented in this paper. Surface diffusion is neglected since its contribution to the overall transport cannot be assessed precisely. Binary gas mixtures only are considered.

2.1. Molecular or ordinary diffusion

Molecular diffusion defines the mechanism by which the different species of a mixture move relative to each other under the influence of concentration gradients, and where molecule–molecule collisions dominate over molecule–pore wall collisions, see Fig. 1. This case is encountered when the mean free path λ of gas molecules is much smaller than the characteristic length scale of the pores (the pore diameter if the pores are assumed to be cylindrical). For a binary mixture, in which there is no pressure gradient, the purely diffusive fluxes J_{1D} and J_{2D} in a porous material can be written as:

$$J_{1D} = -D_{12}\nabla_{c_1} \tag{1}$$

$$J_{2D} = -D_{21}\nabla_{c_2} \tag{2}$$

where D_{12} and D_{21} are the gas diffusion coefficients, ∇c_1 and ∇c_2 the concentration gradients of gas species 1 and 2 in the pore volume, such that $D_{12}=D_{21}$ and $\nabla c_1+\nabla c_2=0$. The measurable binary gas diffusion coefficients D_{12} and D_{21} through the porous medium are usually related to the free gas diffusion coefficient $D_{12}^{\text{free}}=D_{21}^{\text{free}}$ of the gas species in open space as follows [7,13]:

$$D_{ij} = \frac{\epsilon_g}{\tau} D_{ij}^{\text{free}} \tag{3}$$

where ϵ_g and τ are respectively the percentage of open pores in which ordinary diffusion can take place (unsaturated and interconnected pores) and the tortuosity, i.e., the average length of the diffusion path in the material. Complex relations based on pore geometrical arguments have been derived for the tortuosity factor, which usually depends on the total porosity and the water saturation of the porous medium [13,14].

The free gas diffusion coefficient D_{12}^{free} in a binary gas mixture at low to moderate pressures is well known and results from the molecular theory of gases. The following approximate expression can be obtained in many textbook on the subject [15,16]:

$$D_{12}^{\text{free}} = 1.858\times10^{-7}\left(\frac{1}{M_1}+\frac{1}{M_2}\right)^{1/2}\frac{T^{3/2}}{P\sigma_{12}^2\Omega_D} \tag{4}$$

with D_{12}^{free} the free gas diffusion coefficient in m^2/s, T the absolute temperature (K), P the pressure of the gas mixture (10^5 Pa), M_i the molecular weight of gas i (g/mol), σ_{12} the characteristic length (Å) and Ω_D, the diffusion collision integral (−). Ω_D can be estimated according to the formulae given in the Appendix. Expression (4) shows that the free gas diffusion coefficient in a binary mixture is inversely proportional to the pressure of the gas mixture, i.e., $D_{12}^{\text{free}}=f(1/P)$. According to Eq. (3), a similar dependency can be expected for the diffusion coefficient D_{ij} through the porous medium in case ordinary diffusion is predominant.

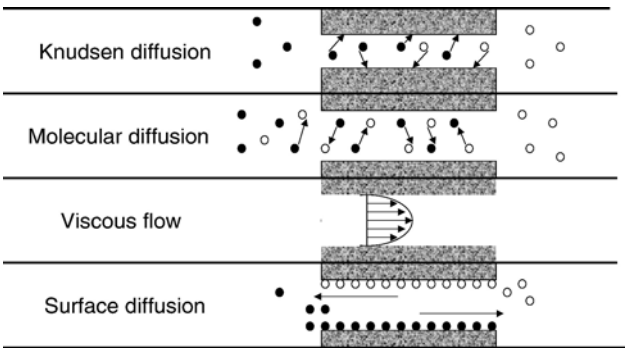

Fig. 1. Transport processes in porous media.

2.2. Free- or Knudsen diffusion

In the free-molecule or Knudsen diffusion mechanism, the gas molecules collide more frequently with the pore walls than with other gas molecules, see Fig. 1. This case is encountered when the mean free path λ of the gas molecules is of the same order as or greater than the characteristic length scale of the pores. Since molecule–molecule interactions are negligible, the Knudsen diffusion flux J_{iD} is independent of the gas

Table 1
Salt solutions and related Relative Humidities

RH (T=20 °C)	54.5%	69.9%	81.8%	93.2%	100%
Salt solution	$Mg(NO_3)_2,H_2O$	KI	KBr	KNO_3	H_2O

composition and is therefore defined for each gas species i by the following relation [7,13]:

$$J_{i\mathrm{K}} = -D_{i\mathrm{K}} \nabla c_i \tag{5}$$

with $D_{i\mathrm{K}}$ the Knudsen diffusion coefficient of gas species i in the porous medium, ∇c_i the concentration gradient of gas species i. Due to the complexity of the geometry of most porous network, attempts have been made to relate the macroscopic Knudsen diffusion coefficient $D_{i\mathrm{K}}$ to that of a single cylindrical pore of average radius r [10,11] (mean radius of the pores in which diffusion can take place, assumed cylindrical and interconnected) through a relation similar to Eq. (3):

$$D_{i\mathrm{K}} = \frac{\epsilon_g}{\tau} D_{i\mathrm{K}}^{\mathrm{pore}} \tag{6}$$

with $D_{i\mathrm{K}}^{\mathrm{pore}}$ the Knudsen diffusion coefficient through a single pore of radius r and ϵ_g/τ the porosity/tortuosity factor previously defined. For a long cylindrical pore, $D_{i\mathrm{K}}^{\mathrm{pore}}$ can be expressed as follows in function of the mean pore radius r and the gas species molecular weight M_i [7,13]:

$$D_{i\mathrm{K}}^{\mathrm{pore}} = \frac{2r}{3}\sqrt{\frac{8RT}{\pi M_i}} \tag{7}$$

with R the ideal gas constant. Note that $D_{i\mathrm{K}}^{\mathrm{pore}}$ is independent of the pressure of the gas mixture and inversely proportional to $\sqrt{M_i}$. According to Eq. (6), this should also be the case for the Knudsen diffusion coefficient $D_{i\mathrm{K}}$ of a gas species i in the porous medium.

2.3. Combination of diffusion mechanisms for binary mixtures

The combination of ordinary and Knudsen diffusion for a binary mixture of gas species i and j is based on momentum-transfer arguments [7]. The total flux of species i, $J_i = J_{iD} + J_{i\mathrm{K}}$ can be written as:

$$J_i = -D_i \nabla c_i \tag{8}$$

with the combined Knudsen-ordinary diffusion coefficient D_i of species i in the porous material given by:

$$D_i = \left(\frac{1}{D_{i\mathrm{K}}} + \frac{1}{D_{ij}}\right)^{-1} = \frac{\epsilon_g}{\tau}\left(\frac{1}{D_{i\mathrm{K}}^{\mathrm{pore}}} + \frac{1}{D_{ij}^{\mathrm{free}}}\right)^{-1} \tag{9}$$

Relation (9) refers to a parallel model, as indicated in reference [13]. It differs from the approach adopted by Klinkenberg [17,18] to combine Knudsen diffusion and viscous flow (series model).

3. Experimental program

3.1. Materials: characteristics, conditioning and sampling

The experimental program has been carried out on hardened cement pastes made of French Industrial CEM I (OPC) and CEM V (BFS-PFA) cements. Cement pastes were preferred to concretes or mortars for the following reasons: diffusion tests in cement pastes can be performed in limited time since thin specimen can be used without experiencing huge size effects, cement paste usually contributes for the greatest part of the porosity of mortars and ordinary concretes and hence determines to a great extent their diffusion properties. Six cylindrical probes (40 mm in diameter and 80 mm long) per cement type (CEM I and V) and w/c ratio (0.35 and 0.45) have been prepared in 1994. After demoulding, they have been cured at 20 °C for 9 months in a $Ca(OH)_2$ water saturated solution. After this period, they have been kept for almost 10 years in sealed dessicators where the Relative Humidity (RH) was controlled by saturated salt solutions, as indicated in Table 1. To study the diffusion properties of the "dry" materials, one probe of each hardened cement paste has been kept in sealed dessicators containing silica gel (RH ≈ 3%). In 2003, the central part of the probes were cut in 20 mm thick slices, three per probe. The end parts of the probes, 10 mm thick, were also kept in order to estimate the total porosity, the wet density and the moisture content of the cement pastes samples. The porosity has been measured by complete drying at 60 °C and re-saturation of the samples at atmospheric pressure. The main physical properties of the studied cement pastes are given in Table 2. After the sawing operation and before testing, the 10 and 20 mm thick samples have been re-conditioned in the same atmospheric conditions as before sawing.

3.2. Experimental set-up

The main element of the experimental set-up is the diffusion cell, as shown in Fig. 2. It consists of two stainless steel compartments of equal dimensions (internal diameter 60 mm, internal length 90 mm, total volume of about 90 ml), separated by the cement paste sample, glued with an epoxy to two half stainless steel rings. The ring system is designed to ensure the gas tightness on the outer surface of the cement paste sample. To this end, it covers partly the flat faces of the cement paste samples, leaving a diffusion surface of 20 mm in diameter, see Fig. 2. The air tightness of the cell is ensured by rubber O-rings which are in contact with the two steel rings.

The experimental set-up used for the diffusion tests, as sketched in Fig. 3, consists of a diffusion cell, vacuum pumps,

Table 2
Properties of the tested cement paste materials

Cement type	CEM I	CEM I	CEM V
w/c ratio	0.35	0.45	0.45
Wet density (g/cm^3)	2.08	2.0	1.92
Porosity (water)	27%	34%	35%

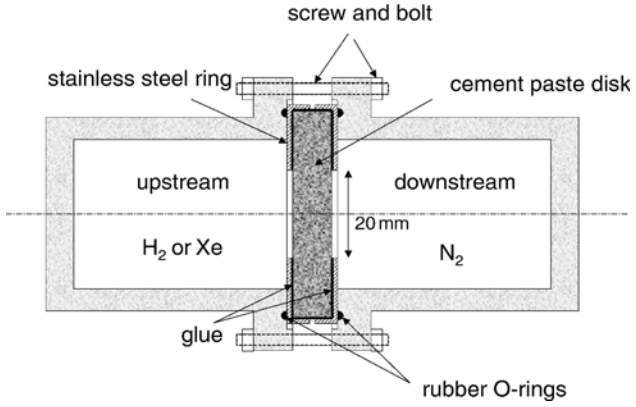

Fig. 2. Sketch of the diffusion cell.

pressure sensors, gas flow lines and a chromatograph. The vacuum pumps are used at the beginning of the test to eliminate the gas phase initially in the diffusion cell and in the gas flow lines. The pressure sensors are used to control and monitor during the test the pressure of the gas mixture in the two compartments of the diffusion cell. The chromatograph is used to analyze periodically the gas mixture in one of the two compartments.

A diffusion test comprises the following steps. The vacuum is first made in the two compartments of the diffusion cell and in the gas flow lines by lowering the pressure to a few mbars for less than a minute. One compartment is then filled with pure hydrogen or xenon, the other with pure nitrogen. The filling-up of the compartments is performed simultaneously by a manual control of the gas inlet using the gas pressure vessels regulators. Once the pressure in the two compartments reaches the target value, the gas flow lines connecting the pressure vessels to the diffusion cell are closed. Periodic analyses of the gas mixture in the nitrogen compartment are then realized. To this end, the gas mixture is allowed to expand in the gas flow lines connecting the nitrogen compartment of the diffusion cell to the chromatograph. When the pressure is stabilized (after a few seconds), a very small volume of gas is sampled and analyzed by the chromatograph. The nitrogen compartment–chromatograph gas flow lines are then immediately closed. Since an analysis results in a small gas expansion due to the non-negligible volume (a few percent of the compartment volume) of the gas flow lines situated between the nitrogen compartment and the chromatograph, the nitrogen compartment is immediately re-filled with pure nitrogen after each measure. This ensures that the gas pressure in the two compartments remains equal during the test. Gas analyses are performed till the steady diffusion state is reached.

The duration of a diffusion test depends on the initial water content of the cement paste sample. For saturated samples, it can last several months. For dry samples, the steady state is usually reached within less than an hour. The mass of the samples (glued in their stainless steel rings) is measured before introducing them in the diffusion cells and at the end of the diffusion test (after taking the cells to pieces). The small mass variations of the samples during the tests are indicated in the presentation of the test results in Section 4 and expressed as variations of the water saturation. These variations take into account the drying of the samples during the vacuum phase. Note that the test is designed to reduce as much as possible the renewing of the gas mixtures in both compartments and hence the drying of the samples: between two gas analyses, the system is closed, there is no renewing of the gas mixtures in both compartments of the diffusion cell. The potential drying of the samples is therefore not related to the test duration, but to the number of measures since a few percent of the gas mixture contained in the nitrogen compartment is lost after each measure (and replaced by dry nitrogen). Between 5 and 10 chromatograph analyses are usually necessary to estimate the diffusion coefficient. This small number of measures is therefore not sufficient to induce a pronounced drying of the samples during the test.

Two VARIAN 3400 chromatographs are used for the gas analyses: one with argon as the carrier gas (for the nitrogen–hydrogen gas mixture) and one with helium (for the nitrogen–xenon gas mixture). The change in carrier gas is made to increase the sensitivity of the measures. A molecular sieve is used to remove moisture from the gas mixtures before passing through the capillary columns of the chromatographs for separation. The operating temperature of the chromatographic ovens is of 180 °C, which allows to perform analyses in less than 10 min. The chromatographs use thermal conductivity detectors to identify and quantify the elements of the gas mixture. Since the identification is not limited to nitrogen, hydrogen and xenon, any lack of air tightness in the diffusion cell is immediately seen through the detection of small quantities of oxygen. For the gas species of interest (hydrogen, xenon), a precise calibration of the thermal conductivity detectors is made prior to the tests which allows for the quantification of very small percentage in the gas mixture (as low as 0.01%).

3.3. Measurement of the diffusion coefficient

Gas analyses in the nitrogen compartment are performed regularly till the steady diffusive flow is obtained. The analyses

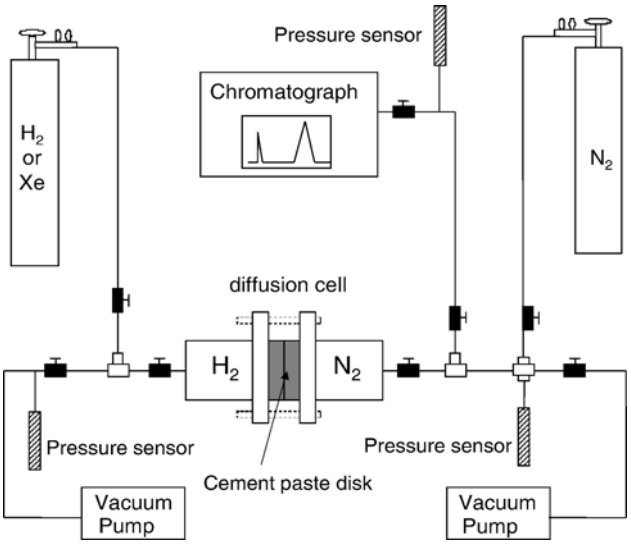

Fig. 3. Sketch of the experimental set-up used for the diffusion tests.

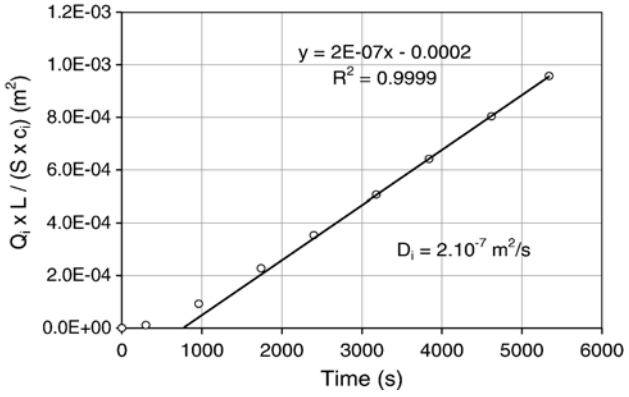

Fig. 4. Estimation of the diffusion coefficient from experimental results (Q is the quantity of H_2 that has passed through a cement paste sample of cross-sectional surface area S and thickness L, c_i^o is the initial H_2 concentration in the upstream compartment of the diffusion cell).

give access to the evolution in time of the quantity of hydrogen (or xenon) that has passed through the cement paste sample, $Q_i(t)$ with i=H_2 or Xe. Considering one-dimensional diffusion through a cement paste sample of thickness L, and using the steady state assumption, Eq. (8) for the total diffusive flux of a gas species i can be re-cast as follows:

$$J_i = -D_i \frac{c_i^u(t) - c_i^d(t)}{L} \tag{10}$$

with $c_i^u(t)$ and $c_i^d(t)$ respectively as the concentration of gas species i in the upstream and downstream compartments of the diffusion cell. At the beginning of the diffusion test, the upstream compartment is filled with the gas species i (H_2 or Xe), and hence $c_i^u(t=0)=c_i^o$. The downstream compartment is filled with nitrogen and hence c_i^d $(t=0)=0$. The test is then performed till steady state is reached. This is usually achieved for small concentrations of gas species i (less than 5%) in the downstream compartment of the diffusion cell. Hence the change in concentration gradient during the test can be neglected:

$$c_i^u(t) - c_i^d(t) \approx c_i^u(t=0) - c_i^d(t=0) = c_i^o \tag{11}$$

Integration in time of Eq. (10) with the condition (11) leads to the following expression for the quantity of gas species i that has passed through the cement paste sample:

$$Q_i(t) = \frac{Sc_i^o}{L} D_i t \tag{12}$$

with S the cross-sectional surface area of cement paste available to gas diffusion. By plotting $Q_i \times L/S/c_i^o$ in function of time as obtained from the periodic gas analyses, it is then possible to estimate the combined Knudsen-ordinary diffusion coefficient D_i, as shown in Fig. 4. Linear regression is used to best-fit the experimental data. Only the last 5–6 points are used since the first measures are characteristic of the transient regime. This method is valid only for gases which are inert with respect to the cement paste. This is the case of hydrogen, xenon, and nitrogen.

4. Experimental results and discussion

4.1. Impact of w/c ratio and cement type on hydrogen diffusion

All the diffusion tests presented hereafter have been performed with a hydrogen–nitrogen gas mixture at a total pressure of 100 kPa. The hydrogen diffusion coefficients measured on the three cement pastes, i.e., the CEM I with w/c ratios equal to 0.35 and 0.45 and the CEM V with w/c=0.45, pre-conditioned in specific atmospheric conditions (3, 55, 70, 82 and 93% RH) are respectively given in Tables 3, 4 and 5 together with the corresponding water saturations (note that the water saturations indicated have been measured on the end parts of the probes, kept in the same hygral conditions). In general, three measures per cement type and hygral condition (RH) have been made. Tables 3, 4 and 5 also present the variations in water saturation of the samples during the diffusion tests (in parentheses). These variations have been obtained by dividing the mass loss of the samples by the average total water content of the saturated samples. As expected from the test method, drying of the samples during the diffusion tests is kept to a minimum, with variations of the water saturation not exceeding 2% and much less than 1% in most cases.

The hydrogen diffusion coefficients of the two CEM I and of the CEM V cement pastes are plotted in Fig. 5 as a function of the water saturation. The continuous lines of Fig. 5 join the average diffusion coefficients obtained for each cement paste and hygral condition.

The shape of the curves obtained for the two CEM I cement pastes are similar. First, they present a plateau for water saturations between 0 and 55–60%. The mean diffusion coefficient is close to 10^{-6} m^2/s in this range. The plateau is followed by a considerable decrease of the diffusion coefficient till water saturations of 80–90% (average diffusion coefficients of about 10^{-10} m^2/s). A greater discrepancy in the experimental results is observed for the CEM I w/c=0.35 samples kept at 82 and 93% RH, see Table 3. No direct trend with the mass losses (ΔS_w) is visible, as shown by Table 3. This indicates that drying of the samples during the tests is not at the origin of this discrepancy. Furthermore, such a dispersion in test data is not observed for the CEM I w/c=0.45 cement paste samples kept at 82 and 93% RH, see Table 4, in spite of similar variations of the water saturation during the tests. The scattering of the CEM I $w/$

Table 3
Hydrogen diffusion coefficients $D^i_{H_2}$(m^2/s) with i the sample number, water saturation S_w and variations of the water saturation ΔS_w during the diffusion tests for the CEM I cement paste samples with an 0.35 w/c ratio (total pressure 100 kPa)

RH (%)	3	55	70	82	93
S_w (%)	5.6	59.1	74.6	91.5	95.6
$D^1_{H_2}$(m^2/s)	9.4 10^{-7}	6.8 10^{-7}	5.1 10^{-8}	2.0 10^{-11}	6.1 10^{-12}
ΔS_w (%)	(0.15)	(0.15)	(0.59)	(1.9)	(0.74)
$D^2_{H_2}$(m^2/s)	8.4 10^{-7}	8.0 10^{-7}	3.1 10^{-8}	2.5 10^{-12}	1.6 10^{-11}
ΔS_w (%)	(−0.15)	(0.15)	(0.3)	(1.6)	(0.59)
$D^3_{H_2}$(m^2/s)	8.0 10^{-7}	8.5 10^{-7}	3.3 10^{-8}	1.6 10^{-10}	2.3 10^{-10}
ΔS_w (%)	(0.44)	(0.)	(0.44)	(0.3)	(0.59)
D_{H_2}(m^2/s) average	8.6 10^{-7}	7.8 10^{-7}	3.8 10^{-8}	6.1 10^{-11}	8.4 10^{-11}

Table 4
Hydrogen diffusion coefficients $D^i_{H_2}$(m^2/s) with i the sample number, water saturation S_w and variations of the water saturation ΔS_w during the diffusion tests for the CEM I cement paste samples with an 0.45 w/c ratio (total pressure 100 kPa)

RH (%)	3	55	70	82	93
S_w (%)	1.7	56	63	83.3	97.6
$D^1_{H_2}$(m^2/s)	1.3 10^{-6}	1.7 10^{-6}	7.3 10^{-7}	6.5 10^{-10}	1.3 10^{-10}
ΔS_w (%)	(0.)	(0.12)	(0.35)	(1.2)	(0.94)
$D^2_{H_2}$(m^2/s)	cracked	1.6 10^{-6}	5.4 10^{-7}	2.9 10^{-10}	1.3 10^{-10}
ΔS_w (%)	(/)	(0.12)	(0.23)	(1.4)	(1.1)
$D^3_{H_2}$(m^2/s)	1.4 10^{-6}	1.4 10^{-6}	4.7 10^{-7}	1.2 10^{-10}	1.4 10^{-10}
ΔS_w (%)	(0.)	(0.12)	(0.35)	(0.94)	(0.82)
D_{H_2}(m^2/s) average	1.4 10^{-6}	1.6 10^{-6}	5.8 10^{-7}	3.5 10^{-10}	1.3 10^{-10}

c=0.35 diffusion coefficients is probably due to the increasing importance of any heterogeneity on diffusion when the size of the pore network is reduced and when the pore network is close to full saturation. In this respect, the tests performed on nearly saturated CEM I samples (kept at 100% RH) showed an even greater dispersion, leading diffusion coefficients varying between 10^{-11} and 10^{-13}–10^{-14} m^2/s. These data have not been included in the presentation of the test results since the 10^{-13}–10^{-14} m^2/s diffusion coefficients are based on hydrogen quantities at the limit of resolution of the technique (0.01%).

The porosity of OPC pastes (CEM I) can usually be split up in two major components : the capillary porosity (pore diameters in the 0.01–10 μm range), which depends strongly on the w/c ratio and the microporosity, associated with the C–S–H gel. The C–S–H gel porosity, being closely related to the C–S–H internal structure, is known to vary little with the w/c ratio [19,20]. According to water vapour desorption test results [20], the capillary porosity is first desaturated when the RH decreases from 100% till 40–50%. For lower RHs, it is essentially the micropores which are desaturated [19,20]. A careful comparison of the average diffusion coefficients of Tables 3 and 4 indicates that, for RHs greater or equal to 55%, the diffusion coefficients of the CEM I, w/c=0.45 cement paste are 2 to 8 times greater than that of the CEM I, w/c=0.35 cement paste. The plots of Fig. 5 show on the contrary that the curves for the two CEM I cement pastes are very close when plotted in function of the water saturation. This indicates that a greater desaturation of the pores in the case of the w/c=0.45 cement paste samples is at the origin of the differences in the average diffusion coefficients observed when the materials are in equilibrium with moist air at 93%, 82%, 70% and 55% RH. This is furthermore consistent with the greater total (or capillary) porosity of the CEM I w/c=0.45 cement paste. Surprisingly, the desaturation of C–S–H pores, which represent a considerable part of the total porosity (usually around 50%), does not lead to an increase of hydrogen diffusivity in the cement paste, as shown by the plateau obtained for water saturations in the range 3–60%, see Fig. 5. This result can possibly be explained by the small size of the C–S–H pores (1–3 nm in diameter) which may make them improper to gas diffusion, or by the important porous network that is already available to gas diffusion as a result of the desaturation of capillary pores.

The impact of the pore size distribution on hydrogen diffusion can further be stretched by comparing the results obtained for the CEM I (OPC) and CEM V (BFS-PFA) cement paste samples. It should be recalled that, in spite of their relatively close total porosities (see Table 2), the pore spaces of the two cement pastes are known, according to microstructural studies, permeability tests [21,22], and radionuclides diffusion tests [23], to be very different. In particular, MIP (Mercury Intrusion Porosimetry) test results show that the percolation threshold (i.e. the greatest mercury accessible pore diameter) for CEM V cement pastes is much smaller than for CEM I cement pastes (i.e., it is necessary to apply much higher mercury pressures to CEM V cement pastes for mercury to first intrude the sample). The percolation threshold is usually considered as an indicator of the minimum dimension of an interconnected capillary network in the material [24]. Furthermore, the capillary porosity of mature CEM V cement pastes is usually thought to be markedly discontinuous [25].

The CEM I and CEM V curves of Fig. 5 (w/c=0.45) present a plateau for water saturations between 0 and 60%. The mean hydrogen diffusion coefficients for the two materials are however very different at this stage, being equal to 1.4 10^{-6} m^2/s and 7.5 10^{-8} m^2/s, respectively. For the CEM I material, the plateau is followed by a regular decrease of the diffusion coefficient by 4 orders of magnitude till water saturations of 80%–90% (average value of about 10^{-10} m^2/s). For the CEM V cement paste, the evolution of the diffusion coefficient for

Table 5
Hydrogen diffusion coefficients $D^i_{H_2}$(m^2/s) with i the sample number, water saturation S_w and variations of the water saturation ΔS_w during the diffusion tests for the CEM V cement paste samples with an 0.45 w/c ratio (total pressure 100 kPa)

RH (%)	3	55	70	82	93
S_w (%)	6.2	58.6	75.6	87.7	90.4
$D^1_{H_2}$(m^2/s)	4.4 10^{-8}	cracked	3.9 10^{-9}	5.5 10^{-9}	6.3 10^{-12}
ΔS_w (%)	(1.5)	(/)	(0.)	(0.11)	(0.22)
$D^2_{H_2}$(m^2/s)	7.0 10^{-8}	1.5 10^{-8}	3.5 10^{-9}	5.1 10^{-9}	not measured
ΔS_w (%)	(−0.11)	(0.79)	(0.)	(0.)	(/)
$D^3_{H_2}$(m^2/s)	1.1 10^{-7}	4.4 10^{-8}	7.6 10^{-9}	2.8 10^{-9}	8.3 10^{-14}
ΔS_w (%)	(−0.11)	(0.79)	(0.)	(0.)	(/)
D_{H_2}(m^2/s) average	7.5 10^{-8}	3.0 10^{-8}	5.0 10^{-9}	4.5 10^{-9}	2.1 10^{-12}

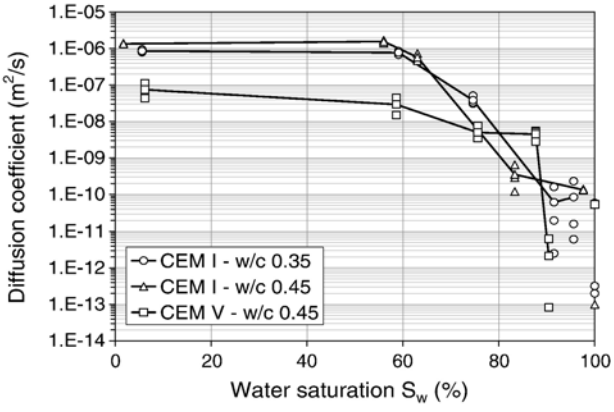

Fig. 5. Hydrogen diffusion coefficients versus water saturation for the CEM I (w/c=0.35 and 0.45) and CEM V (w/c=0.45) cement paste samples.

water saturations between 60% and 85% is very slow, decreasing by only one order of magnitude (leading a mean diffusion coefficient of 5.10^{-9} m^2/s at a water saturation of 87%). From this point on, Fig. 5 indicates that a small variation of the water saturation (from 87% to 90%) leads to a sharp decrease of the diffusion coefficient by three orders of magnitude (leading a mean diffusion coefficient of 2.1 10^{-12} m^2/s at S_w=90%). Measures made on nearly saturated samples (kept at 100% RH) indicate a further decrease of the hydrogen diffusion coefficient in both materials. In particular, no hydrogen flow has been observed during two of the three 7-months long diffusion tests performed on the CEM V samples.

The impact of pore connectivity on gas diffusion in cement paste can first be outlined by comparing the diffusion coefficients obtained on the dry CEM I and CEM V samples, see the 3% RH column in Tables 4 and 5. Diffusion of hydrogen in the dry CEM V cement paste is almost 20 times slower than in the dry CEM I cement paste. Since the evolution of the diffusion coefficients between the dry state and 55% RH (i.e., $0<S_w<60\%$) is very small for both cement pastes (RH range where the micropores are desaturated), these results can be attributed to main differences in the capillary pore system of the two cement pastes. The sharp decrease of the CEM V diffusion coefficient that can be seen by comparing the measures obtained on the samples kept at 82 and 93% RH, see Table 5, is a second indication of the discontinuity of the capillary pore system in the CEM V cement paste. Similar in some sense to a percolation threshold, it shows that, above a given water saturation (here 90%), the pore network of the CEM V cement paste accessible to gas species becomes highly discontinuous [21]. This behaviour is not observed for the CEM I cement paste which presents a continuous evolution of the diffusion coefficient for water saturations between 60% and 90%. This difference could originate from a more uniform pore size distribution in CEM V cement pastes, centered on smaller pore diameters, as shown for example by mercury intrusion porosimetry [22]. The diffusion threshold would then be related to the saturation of an important fraction of the pores of similar diameter. The wider pore size distribution in CEM I cement pastes would, on the contrary, lead a smoother evolution of the diffusion coefficient since the saturation (or desaturation) of the pore system would occur progressively.

4.2. Impact of the gas molecular weight on gas diffusion in cement paste

To study the impact of the gas molecular weight on gas diffusion in cement pastes, diffusion tests have been performed on the CEM I w/c=0.45 cement paste samples with hydrogen–nitrogen and xenon–nitrogen gas mixtures. Xenon was selected because of its high molecular weight and atomic radius (respectively 131 g/mol and 131 pm) as compared to hydrogen (respectively 2 g/mol and 37 pm). According to Eq. (4), the free diffusion coefficient of xenon in nitrogen at 100 kPa is equal to 1.24 10^{-5} m^2/s. That of hydrogen in nitrogen at the same pressure is equal to 7.53 10^{-5} m^2/s (see the Appendix for the application of Eq. (4) to hydrogen–nitrogen and xenon–nitrogen gas mixtures). In theory, if ordinary diffusion predominates and if the porosity/tortuosity factor is the same for xenon and hydrogen, then the xenon to hydrogen diffusion coefficient ratio in cement paste equals that of the same gas species in open space:

$$\frac{D_{Xe}}{D_{H_2}} = \frac{D^{free}_{Xe/N_2}}{D^{free}_{H_2/N_2}} = \frac{1.24\ 10^{-5}}{7.53\ 10^{-5}} = 0.165 \quad (13)$$

Applying in the same manner Eqs. (6) and (7) to xenon and hydrogen, the xenon to hydrogen diffusion coefficient ratio in cement paste, in case Knudsen diffusion predominates, is given by:

$$\frac{D_{Xe}}{D_{H_2}} = \sqrt{\frac{M_{H_2}}{M_{Xe}}} = \sqrt{\frac{2}{131}} = 0.124 \quad (14)$$

Note that the diffusion coefficients ratios of Eqs. (13) and (14) are close.

The diffusion tests have been performed first with hydrogen–nitrogen and then with xenon–nitrogen. The experimental xenon and hydrogen diffusion coefficients obtained from the tests are given in Table 6, together with the variations in water saturation during the tests. In a few cases, a second hydrogen–nitrogen diffusion test has been undertaken after the xenon–nitrogen test (see the lines D_{H_2} bis in Table 6). The average hydrogen (based on the two test series) and xenon diffusion coefficients for each conservation conditions are also indicated in Table 6, together with the average xenon to hydrogen

Table 6
Xenon D^i_{Xe} and $D^i_{H_2}$ hydrogen diffusion coefficients with i the sample number ($D^i_{H_2}$ bis for the second hydrogen test which has been performed after the xenon diffusion test), water saturation S_w and variations in the water saturation ΔS_w during the diffusion tests performed on the CEM I w/c=0.45 cement paste samples (total pressure 100 kPa), average xenon ($D^{average}_{Xe}$) and hydrogen ($D^{average}_{H_2}$) diffusion coefficients, average xenon to hydrogen diffusion co efficients ratio D_{Xe}/D_{H_2} and related standard deviation σ D_{Xe}/D_{H_2} for the different RH conditions

RH (%)	3	55	70	82	93
S_w (%)	1.7	56	63	83.3	97.6
$D^1_{H_2}$(m^2/s)	1.3 10^{-6}	1.7 10^{-6}	7.3 10^{-7}	6.5 10^{-10}	1.3 10^{-10}
ΔS_w (%)	(0.)	(0.12)	(0.35)	(1.2)	(0.94)
$D^1_{H_2}$ bis (m^2/s)	//	2.45 10^{-6}	8.6 10^{-7}	1.05 10^{-9}	//
ΔS_w (%)	(/)	(0.35)	(0.12)	(0.)	(/)
D^1_{Xe} (m^2/s)	//	2.0 10^{-7}	7.2 10^{-8}	1.2 10^{-10}	8.6 10^{-12}
ΔS_w (%)	(/)	(0.)	(0.12)	(0.)	(1.2)
$D^2_{H_2}$ (m^2/s)	Cracked	1.6 10^{-6}	5.4 10^{-7}	2.9 10^{-10}	1.3 10^{-10}
ΔS_w (%)	(/)	(0.12)	(0.23)	(1.4)	(1.1)
$D^2_{H_2}$ bis (m^2/s)	Cracked	2.45 10^{-6}	6.8 10^{-7}	3.9 10^{-10}	//
ΔS_w (%)	(/)	(0.7)	(0.12)	(0.12)	(/)
D^2_{Xe} (m^2/s)	//	1.8 10^{-7}	4.8 10^{-8}	5.8 10^{-11}	6.3 10^{-12}
ΔS_w (%)	(/)	(0.)	(0.12)	(0.12)	(1.4)
$D^3_{H_2}$(m^2/s)	1.4 10^{-6}	1.4 10^{-6}	4.7 10^{-7}	1.2 10^{-10}	1.4 10^{-10}
ΔS_w (%)	(0.)	(0.12)	(0.35)	(0.94)	(0.82)
D^3_{Xe} (m^2/s)	3.0 10^{-7}	1.8 10^{-7}	4.5 10^{-8}	1.1 10^{-11}	6.4 10^{-12}
ΔS_w (%)	(0.)	(0.)	(0.23)	(0.)	(0.82)
$D^{average}_{H_2}$ (m^2/s)	1.3 10^{-6}	1.9 10^{-6}	6.6 10^{-7}	4.5 10^{-10}	1.3 10^{-10}
$D^{average}_{Xe}$ (m^2/s)	3.0 10^{-7}	1.9 10^{-7}	5.5 10^{-8}	6.2 10^{-11}	7.1 10^{-12}
D_{Xe}/D_{H_2} average	0.23	0.1	0.09	0.12	0.05
σ D_{Xe}/D_{H_2}	0.	0.02	0.01	0.05	0.01

diffusion coefficients ratios (D_{Xe}/D_{H_2}). As previously, the variations in the water saturation during the tests remain inferior to 2% and usually far less than 1%. The second hydrogen diffusion tests (named 'bis' in Table 6) performed on some samples show the effect of the small water losses on hydrogen diffusion, with an increase of the diffusion coefficient from 10 to 60%.

The evolution with the water saturation of the xenon diffusion coefficient in the CEM I cement paste is presented graphically in Fig. 6, together with that of the hydrogen diffusion coefficient and the theoretical estimates in case of predominant ordinary (using Eq. (13) and the average hydrogen diffusion coefficients of Table 6) or Knudsen (using Eq. (14) and the average hydrogen diffusion coefficients of Table 6) diffusion mechanisms. Fig. 6 shows that the shape of the curves obtained for xenon and hydrogen are very similar. The measured diffusion coefficients for xenon are overall 5 to 20 times smaller than that of hydrogen.

If one considers all the measures performed on the cement paste samples, the average xenon to hydrogen diffusion coefficients ratio equals 0.11 with a standard deviation of 0.05. This result is close to the theoretical estimate based on Knudsen diffusion (0.124) but the dispersion of the test data is too high to allow one to conclude on the predominance of Knudsen or ordinary diffusion. Furthermore, Fig. 6 shows that the theoretical xenon diffusion coefficients based on both mechanisms describe the experimental results equally well for the entire water saturation range. The results of Table 6 indicate that there is a negligible impact of water saturation on the xenon to hydrogen diffusion coefficient ratio in the 55–82% RH range (average ratios of 0.1, 0.09 and 0.12). This shows that the unsaturated capillary pore space available in this RH range to hydrogen diffusion is also fully accessible to xenon in spite of the greater size of the xenon molecule. At 93% RH, the xenon to hydrogen diffusion coefficient ratio drops to 0.05 with a standard deviation of 0.01. The tests performed on saturated samples (kept at 100% HR) showed an even greater reduction since no xenon flow has been observed during the one year long tests. It seems therefore that the diffusion of xenon in cement pastes compared to that of hydrogen becomes very difficult when the percentage of unsaturated pores diminishes.

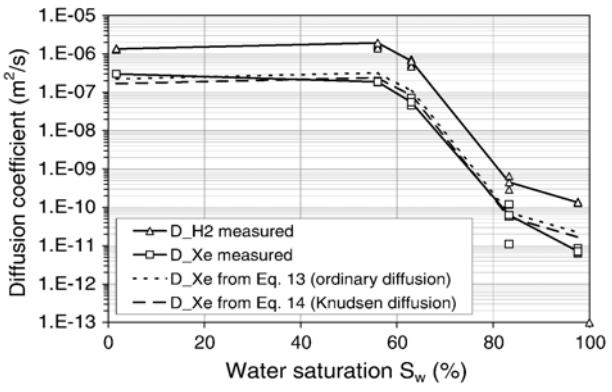

Fig. 6. Hydrogen and xenon diffusion coefficients versus water saturation for the CEM I cement paste samples with a *w/c* ratio of 0.45.

Table 7
Hydrogen diffusion coefficients (m^2/s) obtained on the CEM I cement paste samples tested at 10, 50, 100 and 190 kPa

Pressure (kPa)	10	50	100	190
CEM I *w/c*=0.35 RH 3%	$2.01\ 10^{-6}$	$1.27\ 10^{-6}$	$1.05\ 10^{-6}$	$8.04\ 10^{-7}$
CEM I *w/c*=0.35 RH 55%	$1.72\ 10^{-6}$	$1.41\ 10^{-6}$	$1.18\ 10^{-6}$	$9.07\ 10^{-7}$
CEM I *w/c*=0.35 RH 70%	$7.4\ 10^{-8}$	$7.24\ 10^{-8}$	$5.45\ 10^{-8}$	$4.47\ 10^{-8}$
CEM I *w/c*=0.35 RH 82%	$2.28\ 10^{-10}$	$1.79\ 10^{-10}$	$1.15\ 10^{-10}$	$7.98\ 10^{-11}$
CEM I *w/c*=0.45 RH 3%	$2.31\ 10^{-6}$	$1.39\ 10^{-6}$	$1.08\ 10^{-6}$	$1.09\ 10^{-6}$
CEM I *w/c*=0.45 RH 55%	$3.27\ 10^{-6}$	$2.95\ 10^{-6}$	$2.45\ 10^{-6}$	$1.81\ 10^{-6}$
CEM I *w/c*=0.45 RH 70%	$1.14\ 10^{-6}$	$9.93\ 10^{-7}$	$8.02\ 10^{-7}$	$6.21\ 10^{-7}$
CEM I *w/c*=0.45 RH 82%	$3.64\ 10^{-9}$	$3.52\ 10^{-9}$	$2.69\ 10^{-9}$	$2.70\ 10^{-9}$

These results can possibly be attributed to the formation of discontinuities in the porous network accessible to gas diffusion. When the RH is high, the narrow connections (necks) that exist between large pores which are still unsaturated can be filled with liquid water [5]. Hence, the diffusion of a gas through nearly saturated materials depends on the solubility and on the diffusion coefficient of the gas in the liquid phase that saturates the pore necks. The solubility of xenon in water ($0.11\ m^3/m^3$) is five times greater than that of hydrogen ($0.02\ m^3/m^3$) and cannot therefore explain the lack of xenon diffusion through the nearly saturated CEM I cement paste samples. Its important size (the atomic radius of xenon is 3.5 times greater than that of hydrogen), which would limit its diffusion in saturated narrow pore connections, could however be at the origin of these results.

4.3. Impact of the total gas pressure on gas diffusion

The total gas pressure dependency is one of the major difference that exists between ordinary and Knudsen diffusion in porous media. In case of ordinary diffusion, the diffusion coefficient of a gas species in a porous medium is inversely proportional to the total pressure, see Eqs. (3) and (4). In case of Knudsen diffusion, it does not depend on the total pressure of the gas phase, see Eqs. (6) and (7). To determine which is the dominant diffusion mechanism in cementitious materials, hydrogen diffusion tests have been performed at four different pressures (10, 50, 100 and 190 kPa) on samples of the two CEM I cement pastes in equilibrium with air at 3, 55, 70 and 82% RH. One sample per RH and cement paste type has been tested at the four different pressures in a random order.

The hydrogen diffusion coefficients measured at the four different pressures and on the different cement pastes are given in Table 7. As shown by these results, whatever the RH and the cement paste, the hydrogen diffusion coefficient decreases with increasing pressure. This trend is consistent qualitatively with an ordinary diffusion mechanism. However, quantitatively, the evolution of the hydrogen diffusion coefficient is far from being proportional to $1/P$ for the entire pressure range. This can be best seen by plotting the $D_{H_2}(P)/D_{H_2}(P_o=100\ kPa)$ diffusion coefficient ratio in function of the pressure ratio P_o/P (kPa/kPa), as illustrated in Fig. 7. In case of a purely ordinary diffusion mechanism, $D_{H_2}(P)/D_{H_2}(P_o)=P_o/P$, as shown by the continuous line in Fig. 7. In case of a purely Knudsen

diffusion mechanism, $D_{H_2}(P)/D_{H_2}(P_o)=1$, as indicated by the dashed line in Fig. 7.

Fig. 7 can be split up in two parts. When the pressure exceeds the atmospheric pressure ($P>100$ kPa, $100/P<1$), all the experimental measures (except one point) lie in between the two diffusion mechanisms lines, indicating that neither of them is predominant. The mean diffusion coefficient ratio $D_{H_2}(P)/D_{H_2}$ (100 kPa) for $P=190$ kPa is equal to 0.795 (0.53 would mean that ordinary diffusion is dominant, 1, Knudsen diffusion). On the contrary, when the pressure is below the atmospheric pressure ($P<100$ kPa, $100/P>1$), all the test points (circles and triangles) lie close to the pure Knudsen diffusion mechanism line, indicating that the total pressure of the gas phase has little impact on the hydrogen diffusion coefficient in cement paste. The mean diffusion coefficient ratio $D_{H_2}(P)/D_{H_2}$ (100 kPa) for $P=50$ kPa and $P=10$ kPa are respectively equal to 1.291 (a value of 2 would mean that ordinary diffusion is dominant) and 1.62 (a value of 10 would mean that ordinary diffusion is dominant), therefore very close to 1 (Knudsen diffusion). These results are consistent with the increase of the mean free path of the gas molecules when the pressure of the gas phase diminishes.

Obviously, the pressure dependency of the diffusion mechanism at hand in cement paste does not vary with the hygral state of the cement paste, i.e., its water saturation and hence the RH of equilibrium, see Table 7. This means that it is the same diffusion mechanisms which dominate in cement paste when the capillary pores and/or the micropores are accessible to the gas phase. Classically, one would expect some change of mechanism in relation to the RH of equilibrium, and hence to the size of the unsaturated pores, according to the well-known Kelvin equation. The complex pore connections and tortuosity in cement paste are very probably at the origin of these results. In fact, the diffusion path through cementitious materials can be seen as a succession of meso- and micropores connected by necks which makes therefore the overall gas flow dependent on the size of the smallest pores. Since, as shown in Section 4.1., the desaturation of micropores has no impact on hydrogen diffusion in CEM I cement paste, the pores of interest are not related to the CSH gel but rather to the capillary pore system. This seems consistent with the observed combined mode of diffusion at 190 kPa, which means that the mean free path of the gas molecule (0.05 μm) is of the same order as the pore diameters which control the pressure dependency.

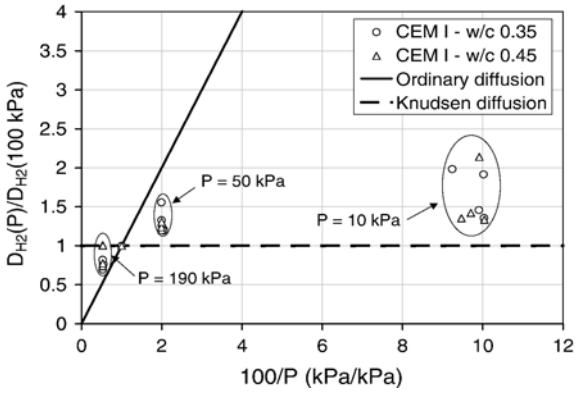

Fig. 7. Hydrogen diffusion coefficients ratio versus total pressure ratio for the tests performed on CEM I and CEM V cement paste samples at 10, 50, 100 and 190 kPa.

Table 8
Lennard–Jones parameters used in Eq. (4) to calculate the free diffusion coefficients of hydrogen and xenon in nitrogen (taken from reference [16])

	M_i (g/mol)	σ_i (Å)	ϵ_i/k (K)
H_2	2.016	2.827	59.7
N_2	28.0	3.568	113.0
Xe	131.3	4.061	225.3

5. Conclusions

In this paper, experimental results on gas diffusion in three cement pastes have been presented. The main conclusions of this study are:

1. Gas diffusion depends essentially on the water saturation of the cement paste (which determines the percentage of pores available to gas), and hence on the RH of air when the material is in equilibrium with its external environment. The hydrogen diffusion coefficient was found to vary between 10^{-6} m^2/s for dry samples and 10^{-10}–10^{-13} m^2/s for nearly saturated samples.
2. The total porosity and the pore size distribution/connectivity of cement paste have a strong impact on hydrogen diffusion. Capillary pores are of great importance with regards to gas diffusion in cementitious materials since the diffusion coefficient decreases strongly in the RH range 55–100%. On the contrary, as shown by the lack of variation of diffusion properties when the RH is smaller than 55%, micropores play a negligible role with regards to gas diffusion in cementitious materials.
3. Gas diffusion in CEM I cement paste depends approximately on the inverse of the square root of the gas molecular weight (relation known as Graham's law for gas species in open space), except when the water saturation of the material is high, i.e., greater or equal to 80–90%. This limit is probably due to the discontinuity of the unsaturated pore network at high RH which makes gas diffusion through nearly saturated cementitious materials dependent on the gas solubility and gas diffusion properties in liquid water.
4. In the pressure range 100–190 kPa, the pressure dependency of the gas diffusion coefficient in CEM I cement paste shows that there are contributions from both ordinary and Knudsen diffusion (i.e., transitional regime). When the pressure is lowered, the contribution of ordinary diffusion tends to decrease and becomes almost negligible at 10 kPa. This result indicates that Knudsen diffusion mechanisms are dominant at small pressures. The water saturation has no impact on these trends. These results need to be confirmed for greater total gas pressures and might not reflect what happens in mortars or concrete where pores of greater size can be expected [10,26].

Appendix A

The methodology and the data used in this paper to calculate the binary free diffusion coefficients (xenon–nitrogen or hydrogen–nitrogen) are summarized in Table 8 and taken from reference [16].

The characteristic length σ_{12} of Eq. (4) has been estimated as follows:

$$\sigma_{12} = \frac{1}{2}(\sigma_1 + \sigma_2) \tag{15}$$

with σ_1 and σ_2 the characteristic length of gas species 1 and 2 in the mixture.

Reference [16] gives the following approximate expression to determine the diffusion collision integral Ω_D:

$$\begin{aligned}\Omega_D = {} & 1.06036 \times (T*)^{-0.1561} + 0.193 \\ & \times \exp(-0.47635T*) + 1.03587 \\ & \times \exp(-1.52996T*) + 1.76474 \\ & \times \exp(-3.89411T*)\end{aligned} \tag{16}$$

with

$$T* = \frac{kT}{\epsilon_{12}} \tag{17}$$

and

$$\frac{\epsilon_{12}}{k} = \left[\left(\frac{\epsilon_1}{k}\right)\left(\frac{\epsilon_2}{k}\right)\right]^{1/2} \tag{18}$$

In Eqs. (17) and (18), k is the Boltzmann constant (J/K), T the absolute temperature (K), ϵ_1 and ϵ_2 the characteristic energies of gas species 1 and 2 (J).

References

[1] A.V. Saetta, B.A. Schrefler, R.V. Vitaliani, The carbonation of concrete and the mechanism of moisture, heat and carbon dioxyde flow through porous materials, Cem. Concr. Res. 23 (1993) 761–772.

[2] T. Chaussadent, State of the art and considerations about the carbonation of reinforced concrete, Etudes et Recherches des Laboratoire des Ponts et Chausses, OA29, Paris, 1999, (In French).

[3] B. Bary, A. Sellier, Coupled moisture-carbon dioxyde-calcium transfer model for carbonation of concrete, Cem. Concr. Res. 34 (2004) 1859–1872.

[4] J.-F. Daian, Transp. Porous Media 3 (1988) 563–589.

[5] Y. Xi, Z.P. Bazant, L. Molina, H.M. Jennings, Moisture diffusion in cementitious materials, Adv. Cem. Based Mater. 1 (1994) 258–266.

[6] M. Mainguy, O. Coussy, R. Eymard, Modelling of isothermal hydric transfers in porous media. Application to the drying of cement-based materials, Etudes et Recherches des Laboratoire des Ponts et Chausses, OA32, Paris, 1999, (In French).

[7] E.A. Mason, A.P. Malinauskas, Gas Transport in Porous Media: the Dusty-Gas Model, Elsevier, Amsterdam, 1983.

[8] K. Kobayashi, K. Shuttoh, Oxygen diffusivity of various cementitious materials, Cem. Concr. Res. 21 (1991) 273–284.

[9] Y. Ohama, K. Demura, K. Kobayashi, Y. Satoh, M. Morikawa, Pore size distribution and oxygen diffusion resistance of polymer-modified mortars, Cem. Concr. Res. 21 (1991) 309–315.

[10] Y.F. Houst, F.H. Wittmann, Influence of porosity and water content on the diffusivity of CO_2 and O_2 through hydrated cement paste, Cem. Concr. Res. 24 (1994) 1165–1176.

[11] A. Sharif, K.F. Loughlin, A.K. Azad, C.M. Navaz, Determination of the effective diffusion coefficient in concrete via a gas diffusion technique, ACI Mater. J. 94 (3) (1997) 227–233.

[12] T. Klink, K. Gaber, E. Schlattner, M.J. Setzer, Characterization of the gas transport properties of porous materials by determining the radon diffusion coefficient, Mat. Struct. 32 (1999) 749–754.

[13] P.C. Carman, Flow of Gases through Porous Media, Butterworths Scientific Publications, London, 1956.

[14] R.J. Millington, Gas diffusion in porous media, Science 130 (1959) 100–102.

[15] R.C. Reid, J.M. Prausnitz, T.K. Sherwood, The Properties of Gases and Liquids, Third Ed.McGraw–Hill, New York, 1977.

[16] J. Gosse, Transport properties of gases at moderate pressures, In Les Techniques de l'Ingénieur, Constantes Physico-Chimiques, K, vol. 425, 2005, (In French).

[17] L.J. Klinkenberg, The permeability of porous media to liquids and gases, API Drill. Prod. Pract. (1941) 200–213.

[18] S.A. Reinecke, B.E. Sleep, Knudsen diffusion, gas permeability, and water content in an unconsolidated porous medium, Water Resour. Res. 38 (12) (2002) 16.1–16.15.

[19] T.C. Powers, T.L. Brownyard, Studies of the physical properties of hardened Portland cement paste, J. Am. Concr. Inst. 9 (22) (1947) 971–992.

[20] V. Baroghel-Bouny, Characterization of cement pastes and concretes: methods, analysis, interpretations, [In French], Doctoral dissertation, Laboratoire Central des Ponts et Chaussées, 1994, Paris.

[21] C. Gallé, J.-F. Daian, Gas permeability of unsaturated cement-based materials: application of a multi-scale network model, Mag. Concr. Res. 52 (4) (2000) 251–263.

[22] C. Gallé, Effect of drying on cement-based materials pore structure as identified by mercury intrusion porosimetry. A comparative study between oven-, vacuum-, and freeze-drying, Cem. Concr. Res. 31 (2001) 1467–1477.

[23] C. Richet, Migration of radioelements within cementitious materials. Impact of leaching on transport mechanism, [In French], Doctoral Thesis, University of Paris XI, 1992.

[24] R.A. Cook, K.C. Hover, Mercury porosimetry of hardened cement pastes, Cem. Concr. Res. 29 (1999) 933–943.

[25] H.F.W. Taylor, Cement Chemistry, 2nd Edition, Thomas Telford, London, 1997.

[26] A.W. Harris, A. Atkinson, P.A. Claisse, Transport of gases in concrete barriers, Waste Manage. 12 (1992) 155–178.